

History, Auxology and Examination

HISTORY

All diagnosis begins with a comprehensive history and examination. This chapter covers general points in the assessment of a child who may have an endocrine disorder; more specific points are included in subsequent sections.

First, explore in detail the presenting complaint as perceived by the parents. If old enough, ask patients whether *they* have any concerns, or whether there is a problem only for other family members or medical personnel.

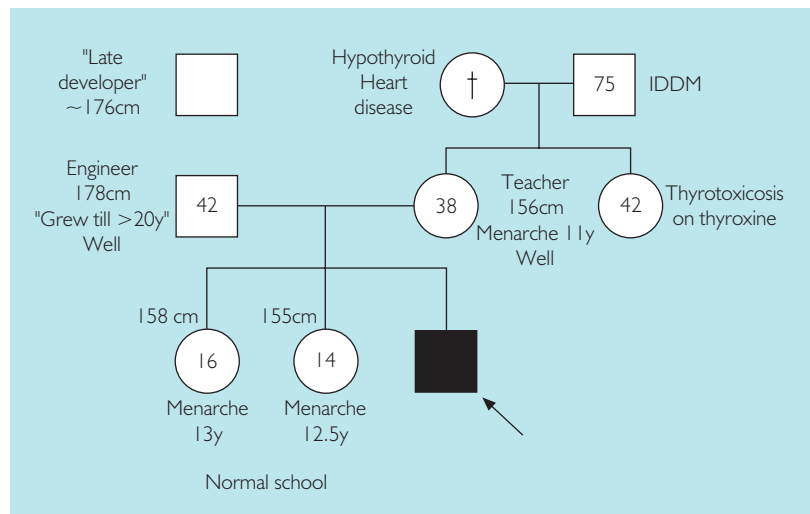
Take details of the mother's pregnancy, including ill health or drug administration (prescribed or illicit), the gestational age, mode of delivery and any requirement for neonatal special care. All mothers can recall the birth weight of their offspring, but it may be possible to obtain birth length and head circumference from parental or hospital records. It is important to obtain information regarding growth rate in height and weight as recorded in past medical records or as perceived by the parents and child – has there been recent gain or loss of weight and is the child growing out of their clothes and shoes before they wear out, or going through a growth spurt?

Establish a family tree that records details of the heights (preferably measured directly), build and age

of sexual maturation of both parents, siblings and any more distant relations with aberrant stature. There is a tendency for both partners to overestimate their own size and for males to underestimate the height of their female partner, with females tending to overestimate their male partner's height. There is a particularly large bias to underestimating weight in familial obesity. Although estimates of predicted height based on reported size are usually a reasonable guide to genetic target height, there can occasionally be huge discrepancies and the measurement of even one parent (usually the mother) increases the accuracy of the prediction. Possible non-paternity (as much as 10% in some studies) should also be borne in mind.

Enquire whether there is parental consanguinity that may lead to an increased risk of autosomal recessive disorders. Ask whether there are any family members with ill health, especially autoimmune (rheumatoid, pernicious anemia, alopecia, vitiligo) or 'gland' problems, and then enquire specifically about thyroid disorders and diabetes mellitus. The pedigree can be used to record social details that may be vitally important when considering both etiology and subsequent treatment and prognosis (**Fig. 1.1**). Is the patient on any regular medication (including topical and inhaled preparations)? Ask about past medical events including

Fig. 1.1 Family pedigree.



- Details of presenting problem and level of concern
- Details of mother's pregnancy and of delivery
- Birth weight and length; other neonatal measurements if available
- Family sizes, ages of sexual maturity
- Family history of endocrine or autoimmune disease
- Social details
- Medication, by any route; past illnesses or operations
- Diet in infancy and current food intake
- Current growth – growing out of clothes or shoes? Make use of any past records of growth
- Developmental or educational level
- Bullying or peer pressure (especially related to size and appearance)
- Any specific symptoms in chest, cardiovascular system, gastrointestinal, CNS, skin

Table 1.1 Essential points in the history

what might be perceived as minor surgical procedures such as hernia repair or orchidopexy. Enquire about the current and early diet, and any specific exclusions.

Depending on the age of the child, establish the developmental or educational level and ask about the ability to participate actively in sport. Is there any bullying from peers? Ask the adolescent about career plans. Finally, run through the other systems of the body not involved in the presenting complaint to exclude other pathology.

The main points that must be established from the history of a child presenting with an endocrine disorder are given in **Table 1.1**.

AUXOLOGY

Detailed measurements can give an immense amount of information when performed and charted properly. **Fig. 1.2** demonstrates the information obtained from each measurement described below.

WEIGHT

This is a deceptively simple measurement, which is often performed very badly. An infant should be weighed naked (**Fig. 1.3**) and a child in the minimal clothing compatible with modesty (**Fig. 1.4**). A wet modern disposable diaper can weigh as much as 450 g (1 lb) and the indoor clothing of a child wearing sports shoes and jeans weighs around 1.5 kg (3 lb 5 oz), contrasted with a mean weight gain in mid-childhood of 2–3 kg (4.5–6.5 lb) per year. All scales should be

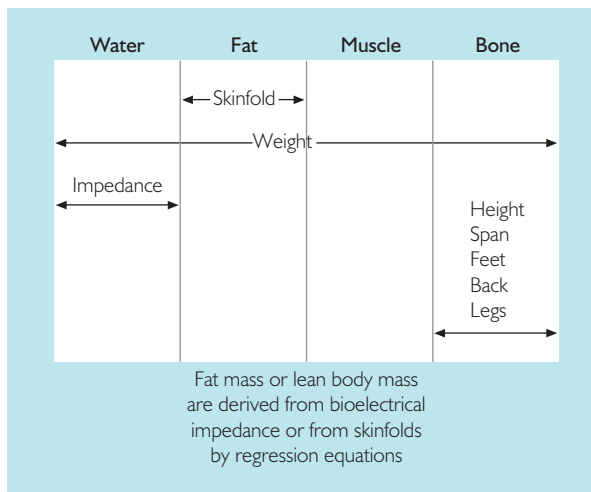


Fig. 1.2 Direct measurements of various body compartments are indicated by the arrows.

calibrated and serviced regularly. A struggling child's weight can be approximated by turning on electronic scales with the mother standing on them – this results in a 'zero' value that changes to the infant's weight when placed in the mother's arms.

LENGTH AND HEIGHT

Under the age of 2 years, and in children with a motor disability, it is usual to record supine length (**Fig. 1.5**). This requires two people, often the mother plus the auxologist. The head is held against the headboard with the face in a horizontal plane. The hips and knees are extended gently and the movable footboard is brought up to touch the soles of the feet held at 90°.

Standing height (**Fig. 1.6**) should be measured using a stadiometer or other rule, in bare feet with the heels in the same vertical plane as the measuring instrument. The arms should be held relaxed at the sides, and the face should be in the 'Frankfurt plane' with the outer canthus and upper ear horizontal. The subject should be asked to take a deep breath in, then out whilst the auxologist exerts *gentle* upward traction on the mastoid processes. It has been shown that the 'stretch' technique, where the traction is sufficient to lengthen the spine slightly, is unnecessary and may result in increased inter-observer error.

Height is read to the nearest complete millimeter at the end of the breath. If repeated measurements of height are taken to establish a growth velocity, then ideally they should be performed at the same time of day to avoid errors due to spinal compression; on average, height measured in the morning is 8 mm (about $\frac{1}{4}$ inch) more than the afternoon value. The

Fig. 1.3 (Right) Measurement of infant weight. The nappy is removed and calibration of the scales checked frequently.

Fig. 1.4 (Far right) Measurement of weight; minimal clothing on calibrated electronic scales.

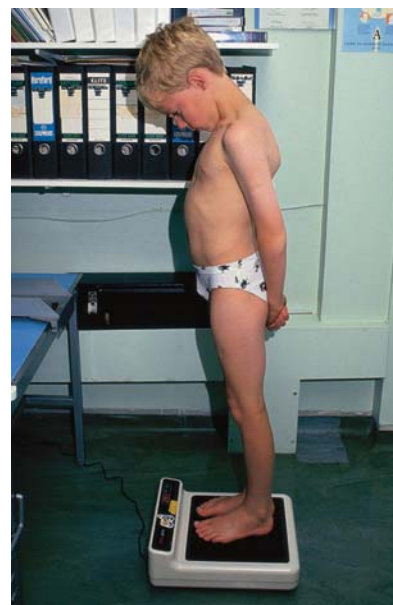


Fig. 1.5 Measurement of infant length. Mother positions head horizontally; auxologist extends legs gently. First, the legs are lifted to reduce the lumbar lordosis and then the heels and feet are slid down the footplate.

Fig. 1.6 Measurement of height, using a gentle stretch technique, with child in bare feet, and a wall-mounted stadiometer.



standard error of measurement of height on a single occasion in the hands of a trained auxologist is in the order of 0.2 cm.

CROWN-RUMP LENGTH OR SITTING HEIGHT

Estimation of the length of the back and head can be of great benefit in establishing the relative proportions of the body. In an infant the legs are drawn up to 90° and the footboard is brought into contact with the

buttocks (**Fig. 1.7**). In an older child, using a specially designed instrument (**Fig. 1.8**) with the feet resting on a bar, the arms folded loosely in the lap and a similar gentle stretch technique to the one described above, it is possible to obtain precise estimates of sitting height. A simpler method uses a hard seat of known height and horizontal top placed under the height stadiometer. Crown-rump length or sitting height may then be subtracted from standing height to derive subischial leg length.



Fig. 1.7 Measurement of infant crown–rump length. First lift the legs to reduce lumbar lordosis and then slide buttocks down the footplate.

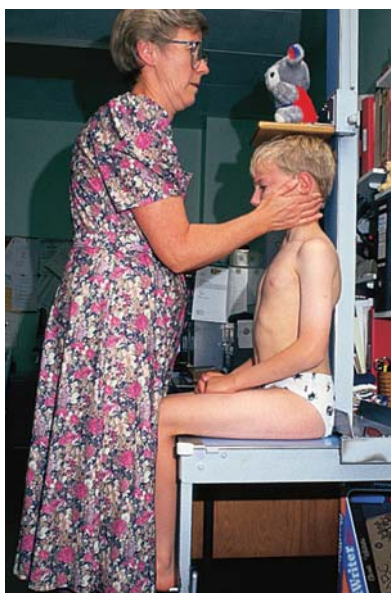


Fig. 1.8 Measurement of sitting height; gentle stretch technique, using purpose-built sitting-height table.

HEAD CIRCUMFERENCE

A non-stretchable paper or metal tape or lasso (e.g. the Lasso-o™ available from the UK Child Growth Foundation) should be used and three estimations made of the maximum occipitofrontal circumference (OFC) (**Fig. 1.9**). In children with abnormal head shape it may not be possible to obtain accurate readings.

SKINFOLD THICKNESS

A skinfold calliper is required that has a known strength of pinch and a known area of tip. Four sites are often chosen, of which the first two are in most common use. The triceps skinfold (**Fig. 1.10**) is



Fig. 1.9 Measurement of head circumference using non-stretchable lasso tape measure (Lasso-o™ Child Growth Foundation, UK).

determined with the left arm loose at the side and a fold raised between the measurer's thumb and forefinger at the mid-point of the dorsum of the upper arm. The callipers are applied and, once the reading has stabilized (4–5 s), the reading is made. The subscapular skinfold (**Fig. 1.11**) is raised at the tip of the shoulder blade, on the left, with the arms again relaxed at the sides. The biceps skinfold (**Fig. 1.12**) is determined as for the triceps skinfold but on the ventral aspect of the upper arm. The suprailiac fold (**Fig. 1.13**) is found at the maximum height of the iliac crest. The skinfold thicknesses give an estimation of the amount of subcutaneous fat, and its distribution, and may be used in various equations to estimate total body adiposity.

ARM AND WAIST/HIP CIRCUMFERENCES

Mid upper arm circumference (MUAC) may be measured using a flexible non-stretch tape measure as means of estimating undernutrition (see Ch. 4) and waist and hip circumferences (then expressed as a waist/hip ratio) as a measure of overnutrition (see Ch. 5).

MUAC is measured at a point half-way between elbow and shoulder (**Fig. 1.14**). Waist circumference is measured between the lower ribs and the ischial ridge, at the level of the umbilicus at the end of a normal expiration. Hip circumference is measured at the level of both greater trochanters.

BODY MASS INDEX

Another commonly used estimate of relative obesity is the body mass index (BMI), or Quetelet index, which can be estimated from the formula: Weight (kg)/Height (m)². BMI varies with age and must be compared with

Figs 1.10–1.13 Measurement of triceps (top left), subscapular (top right), biceps (bottom left) and suprailiac (bottom right) skinfold thickness.

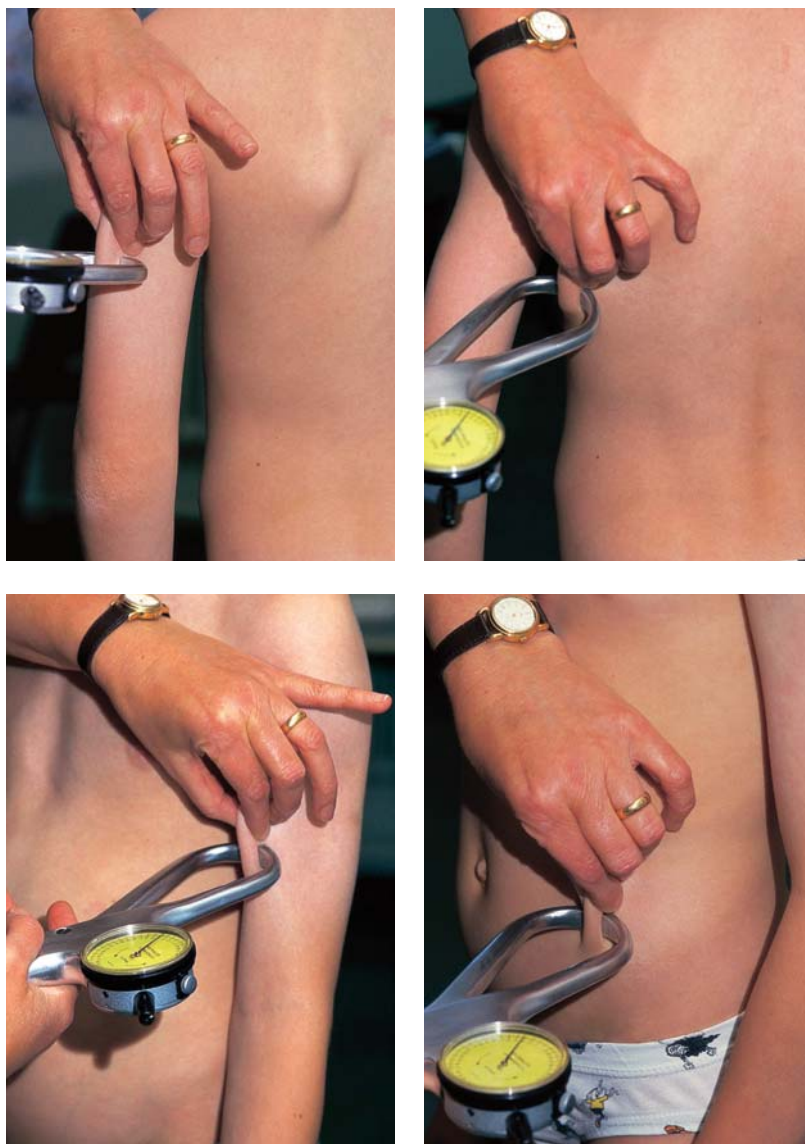


Fig. 1.14 Measurement of mid upper arm circumference, midpoint between elbow and shoulder.

appropriate age- and sex-related standards (see Ch. 5 on The Overweight Child).

OTHER MEASUREMENTS

It is sometimes helpful to assess other body sizes and their relationships directly; standard centile charts exist for almost every imaginable parameter.

Measurement of span is the value most likely to be of use in the endocrine clinic and may be estimated by measuring the fingertip to fingertip distance with the arms held horizontally (**Fig. 1.15**). The normal relationship of span to height is:

$$\text{Span} = \text{Height} \pm 3.5 \text{ cm (1.5 inches)}$$



Fig. 1.15 Measurement of span. The arms are horizontal with the right fingertips held against a fixed vertical bar and the left against a movable vertical guide on calibrated graph paper.



Fig. 1.16 Measurement of individual body segments in a child with short limbs, using an anthropometer.

In short-limbed conditions and if hemihypertrophy is suspected (see below), then direct measurement of limb segments using a specially designed anthropometer (**Fig. 1.16**) or a metal builder's tape measure may be of help.

GROWTH CHARTS

Up-to-date standards for height, weight, BMI and head circumference are available for many populations. Standards should be updated regularly to take secular changes in growth into account, and ideally patients from ethnic subgroups should be compared with appropriate charts, although this is not always possible. Standards for sitting height, leg length, skinfold thickness, span, etc. are less universally available, but published.

Most commonly used charts are sex specific and show the measured parameter on the vertical axis and age on the horizontal. Almost all scales are linear, except for skinfold thickness, where a vertical logarithmic axis is used, and in some charts extending into premature infancy where a non-linear age axis allows expansion of data in the early months.

Many charts use 'centile' lines spaced at varying intervals depending on the design of the chart. A common layout is to use the 0.4th, 2nd, 9th, 25th and 50th centiles with corresponding values above the

mean to give nine centile lines, smoothed by a statistical method known as LMS. Thus only 1 in 250 children would fall below the 0.4th or above the 99.6th centile in a normal population, which may form the basis for a referral protocol.

Charts of height and weight have been published for many named syndromic conditions and should be used where necessary; there are also charts of limb length, height and OFC for many of the skeletal dysplasias.

The measured value should be plotted as a simple dot and other values, such as bone age (see below), plotted in a different color or a square symbol.

Whenever a standard centile chart is used, of whatever construction, it is possible rapidly to estimate the expected genetic potential of the subject by plotting the centile value of each parent on the right-hand y-axis. The mid-parental centile can then be drawn. Alternatively, for height only, the following simple calculations may be performed:

$$\text{Target height of boy in cm} = \frac{(\text{father's height} + \text{mother's height} + 13)}{2}$$

$$\text{Target height of girl in cm} = \frac{(\text{mother's height} + \text{father's height} - 13)}{2}$$

(For imperial units, give height in inches plus a correction of 5 inches.)

If a secular trend is expected, for example if the economic situation of the child is much better than that of the parents in their youth, 4.5 cm (approximately 1.75 inches) should be added to the target height. In 95% of cases the final height of the child is expected to be within the target height ± 9 cm (4.5 inches), the so-called ‘target range’. The centile position of the target height can then be compared with the centile position of the present height of the child. *This is the method used in illustrations throughout this book.*

As growth is a longitudinal process, change of height with time is even more important than absolute height at a particular timepoint. The final evaluation of growth in any parameter is made by connecting consecutive measurements on the growth chart and visually assessing any deviation upwards or downwards through the centile lines.

Growth rate can also be evaluated by calculating a velocity that can be compared with published height and weight velocity curves. Velocity is calculated by the formula:

$$\frac{\text{Ht 2} - \text{Ht 1}}{\text{Interval (decimal/years)}}$$

Because measurement error is magnified when two separately obtained values are used to calculate a velocity (95% confidence interval (CI) for velocity estimated from two measurements 1 year apart = $\pm [2\text{SD of measurement (around 0.25 cm)}] \times \sqrt{2}$; for a 3-month interval the CI is four times this value), the use of this calculation is dependent on accurate measurements and improved by long intervals between estimates. The design of the reference charts means that optimal information will come from yearly estimations of height velocity (and in clinical practice a minimum period of 6 months).

To allow more precise quantification of any normally distributed parameter for which standards exist, it is common to use the Standard Deviation Score (SDS, or Z score), especially for values that lie outside the normal centile range. This technique allows comparison of the parameters for children of different age and sex.

$$\text{SDS} = \frac{x - \bar{x}}{\text{SD}}$$

where x is the measured value; \bar{x} the mean, and SD the standard deviation for a given population. In a normally distributed population the SDS will have a mean of 0 and a SD of 1. A SDS of from -1 to $+1$ includes 68.26%, and from -2 to $+2$ includes 95.44% of

the population. Only 0.13% of a population will have an SDS of more or less than 3. The charts used throughout this book show the mean and ± 1 and 2 SD.

EXAMINATION

The examination of the child can begin during the history-taking by observing their activity, demeanor and interaction with the parents or carers. It is then usual to begin with the hands, work up the arms to the head and neck, examine the chest and back, then the cardiovascular system followed by the abdomen and external inspection of the genitalia with an assessment of maturity. Finish with the central nervous system examination and inspection of the body and skin. These points are now described in more detail.

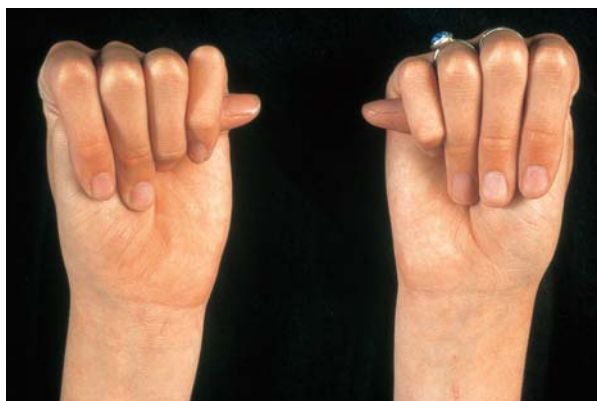
THE HANDS

The hands (and sometimes the feet) hold the clue to many endocrine disorders and syndromic malformations associated with abnormal stature. **Figs 1.17–1.45** show a number of abnormalities with their interpretation.

Abnormal dermatoglyphics (**Fig. 1.17**), such as a single palmar crease, are non-specific signs of possible syndromic malformations. The fingers and wrist may be conveniently used to demonstrate increased mobility and arachnodactyly (**Figs 1.18–1.21**), as may be seen in the Marfan syndrome and some of the collagen disorders, or stiffness in long-standing diabetes mellitus (**Fig. 1.22**) and some of the storage disorders (**Figs 1.23 & 1.24**). Fixed joint contractures, arthrogryposis (**Fig. 1.25**), may be restricted to one group of joints, or may be generalized: it is a non-specific sign of congenital neuromuscular disease and various syndromes. Generally short fingers (brachydactyly) are



Fig. 1.17 Single palmar crease – may be a normal variant but can be a non-specific clue to look for other dysmorphic features.



Figs 1.18, 1.19 Increased joint mobility in the Marfan syndrome shown by touching palm with length of thumb (left) and ability to enclose thumb, which protrudes from the other side, with the clenched hand (above).

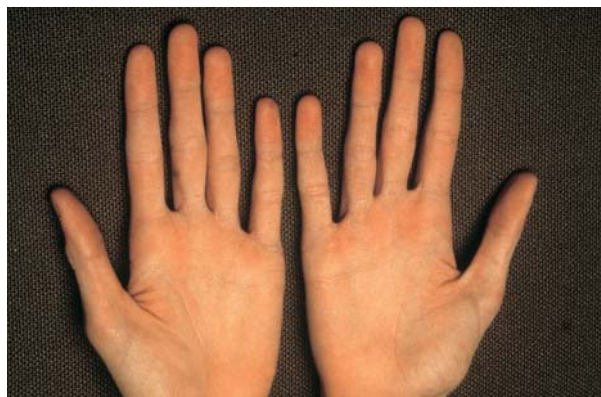


Fig. 1.20 Arachnodactyly in the Marfan syndrome.



Fig. 1.21 The wrist sign, demonstrated by clasping one wrist with the opposite hand and noting overlap of the distal phalanges of thumb and middle finger.

seen in many syndromes associated with short stature (**Fig. 1.26**). Only the fifth finger may be shortened, as in Coffin–Siris syndrome (**Fig. 1.27**), or just one or two metacarpals as in pseudohypoparathyroidism (**Figs 1.28 & 1.29**). Fingers may show fusion (syndactyly), or duplication with or without fusion (polydactyly or polysyndactyly) (**Figs 1.30 & 1.31**), in some dysmorphic syndromes. Polydactyly or other finger abnormalities can be classed as pre-axial (see **Fig. 1.28**) (radial/tibial side) or post-axial (ulnar/fibular) (**Fig 1.32**). All the fingers may be bent, as in various of the

camptodactyly syndromes associated with short stature (**Fig. 1.33**), or just the fifth finger (clinodactyly), which is a non-specific abnormality in many syndromic disorders (**Fig. 1.34**). A trident hand is seen in achondroplasia (**Fig. 1.35**). The thumb may be broad (**Fig. 1.36**), triphalangeal (**Fig. 1.37**) or low set (**Fig. 1.38**) in various syndromes. The fingertips and interphalangeal joints are broad in Aarskog syndrome (**Fig. 1.39**), an X-linked, dominantly inherited, condition associated with moderate short stature. The wrist is expanded in rickets for whatever causes (see



Fig. 1.22 Joint stiffness in a long-standing diabetic. The 'prayer sign' is caused by irreversible glycosylation of tissue proteins (see Ch. 10).



Figs 1.23, 1.24 'Claw hands' in two children with storage disorders: mucopolipidosis 3 (top) and Hunter syndrome (bottom).

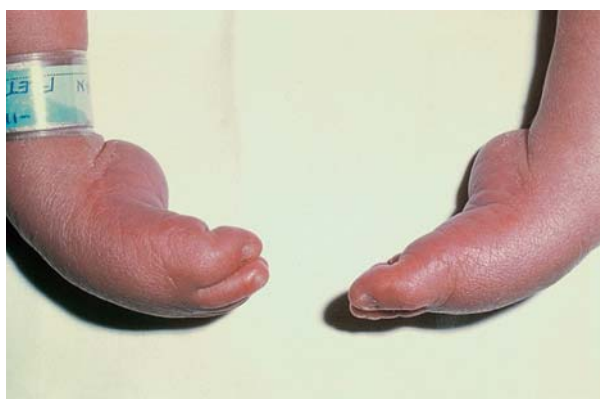


Fig. 1.25 Fixed joint contractures (or arthrogryposis), here presenting as bilateral talipes in a child with camptodactyly and short stature of prenatal onset.



Fig. 1.26 Brachydactyly. This is found in many syndromes associated with short stature.



Fig. 1.27 Isolated short fifth digit in Coffin–Siris syndrome.



Fig. 1.29 Corresponding radiograph of the child in Fig. 1.28.



Fig. 1.28 Short fourth and fifth metacarpals in the hand of child with pseudohypoparathyroidism.



Fig. 1.30 Syndactyly. A common, often familial, variant and a non-specific clue to look for other dysmorphic features. In association with ambiguous genitalia in an XY individual, this may raise the possibility of Smith–Lemli–Opitz syndrome.



Fig. 1.31 Polysyndactyly, here in the Carpenter syndrome.



Fig. 1.32 Post-axial brachydactyly.

Fig. 1.33
Camptodactyly.
There is a group
of camptodactyly
syndromes
associated with
short stature and
scoliosis.

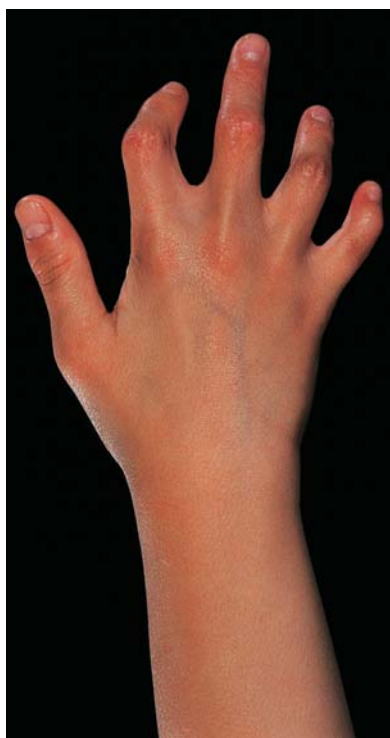


Fig. 1.34 Clinodactyly. This is found in many syndromes associated with short stature.

Fig. 1.35 Trident hand in achondroplasia.



Fig. 1.36 Broad thumb as seen in Rubinstein–Taybi syndrome.



Fig. 1.37
Triphalangeal thumb.



Fig. 1.40 Clubbing, here in a patient with cystic fibrosis.



Fig. 1.38 Low-set thumb.



Fig. 1.41 Deep-set nails in Sotos syndrome.



Fig. 1.39 Expanded interphalangeal joints and fingertips in the X-linked recessive Aarskog syndrome associated with short stature.

Chs 4 & 11). Clubbing is seen in chronic cyanotic heart disease, chronic purulent respiratory disorders and inflammatory bowel disease, as well as occurring dominantly in families (**Fig. 1.40**). The nails may be deep set in the Sotos syndrome of cerebral gigantism (**Fig. 1.41**) and hypoplastic in ectodermal dysplasia and those syndromes characterized by early lymphedema such as the Ullrich–Turner syndrome (**Figs 1.42 & 1.43**). The palms show redness in chronic liver disorders and a yellowish discoloration in true pituitary gigantism (**Fig. 1.44**) and in hypothyroidism, where the knuckles are yellow in contrast to the generalized pallor (**Fig. 1.45**).

THE ARMS

The relative length of the arms can be assessed by measurement of span, as described above. Fixed flexion of the elbow and wrist may be seen with arthrogyriposis, and limited rotation of the forearm in some of the skeletal dysplasias (**Fig. 1.46**). Radial aplasia or hypoplasia and distal digital ray abnormalities may be seen in some dysmorphic short-stature syndromes and

Fig. 1.42

Hypoplastic nails as seen in around 40% of girls with Ullrich–Turner syndrome.

**Fig. 1.45** Extremely pale skin and yellow knuckles in hypothyroidism.**Fig. 1.43** Neonatal lymphedema, as seen in 75% of girls with Ullrich–Turner syndrome.**Fig. 1.44** Yellow palmar discoloration in pituitary gigantism.**Fig. 1.46** Radiograph of forearm in Leri–Weill dyschondrosteosis with bowed radius producing limited forearm rotation – the Madelung deformity.

associated with congenital heart defects, renal or hematologic abnormalities (**Fig. 1.47**). An increased carrying angle (**Fig. 1.48**) is classically seen in the Ullrich–Turner syndrome, although it is absent in 50% of cases and may be present in other syndromes.



Fig. 1.47 Radial hypoplasia and digital ray abnormality in Holt–Oram syndrome, associated with atrial and ventricular septal defects.



Fig. 1.48 Increased carrying angle as seen in 40–50% of girls with Ullrich–Turner syndrome.

THE HEAD AND NECK

There are many abnormalities of this region that may indicate pathology, and a selection of these is given in **Figs 1.49–1.86**.

Redundant skin at the site of previous fetal nuchal edema is a feature of the Down, Ullrich–Turner and other chromosomal syndromes in the neonatal period (**Figs 1.49 & 1.50**) and may be more obvious than webbing at this stage. Webbing of the neck (**Fig. 1.51**) is seen in 70% of cases of Ullrich–Turner syndrome, although it is not a specific finding, and a short neck with a low hairline (**Figs 1.52 & 1.53**) is also seen in many dysmorphic syndromes (**Fig. 1.54**).

The shape of the skull should be assessed. Mild brachycephaly or plagiocephaly is common, but if craniosynostosis (**Figs 1.55 & 1.56**) is suspected there

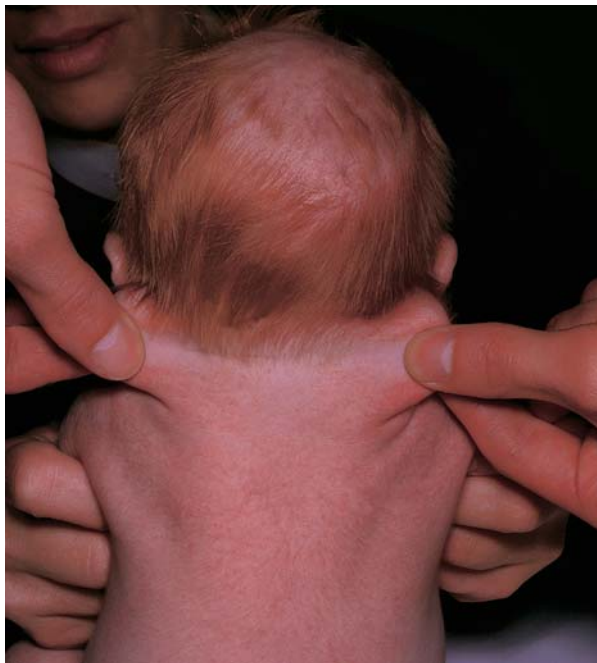


Fig. 1.49 Loose skin of neck in neonate with Down syndrome.



Fig. 1.50 Loose skin of neck in neonate with Ullrich–Turner syndrome.

should be palpable suture lines and a typical radiographic appearance (**Figs 1.57 & 1.58**).

Around the eyes hypertelorism (**Fig. 1.59**), heavy supraorbital ridges (**Fig. 1.60**) or the presence of epicanthic folds, ptosis (**Fig. 1.61**), blepharophimosis, microphthalmia and exophthalmos (**Fig. 1.62**) due to thyrotoxicosis should be assessed. There may be prolapsing of the temporal horn into the orbit, producing exophthalmos in neurofibromatosis (**Figs 1.63 & 1.64**) and syndromes affecting the depth of the orbit such as Apert syndrome.



Fig. 1.51 Later webbing of the neck in a patient with Noonan syndrome (as seen to some degree in 70% of girls with Ullrich–Turner syndrome). Note abnormal ears, seldom seen in Ullrich–Turner syndrome.

Fig. 1.54 Short neck due to vertebral abnormalities (the Klippel–Feil malformation), producing an appearance superficially similar to the webbed neck of Ullrich–Turner syndrome.



Figs 1.52, 1.53 Low hairline with midline extension seen in 75% of girls with Ullrich–Turner syndrome, shown in a neonate (above) and in late childhood (right).

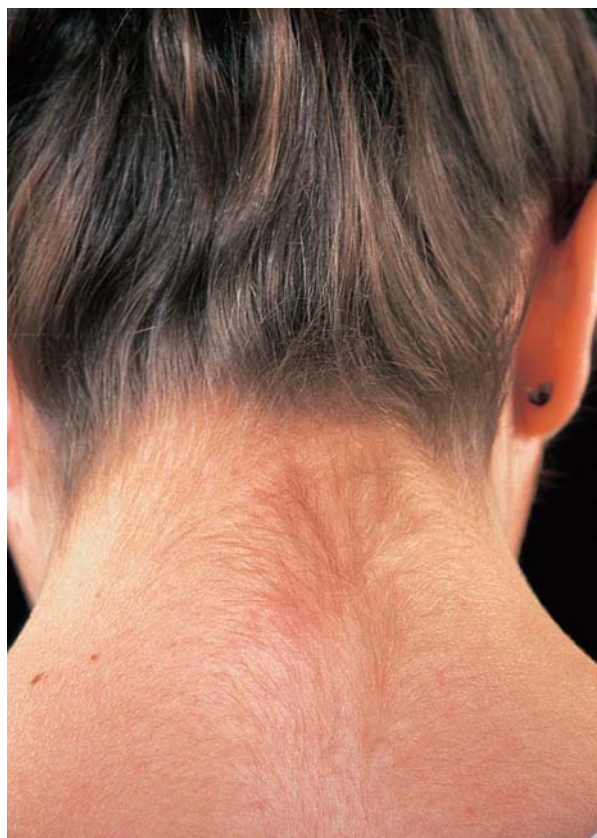




Fig. 1.55 Dolichocephaly from craniosynostosis.

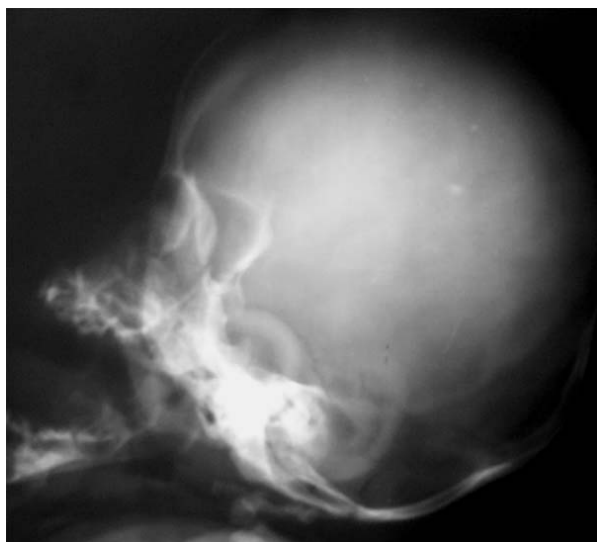


Fig. 1.57 Radiograph of coronal craniosynostosis showing absent suture lines with sclerosis and abnormal head shape.

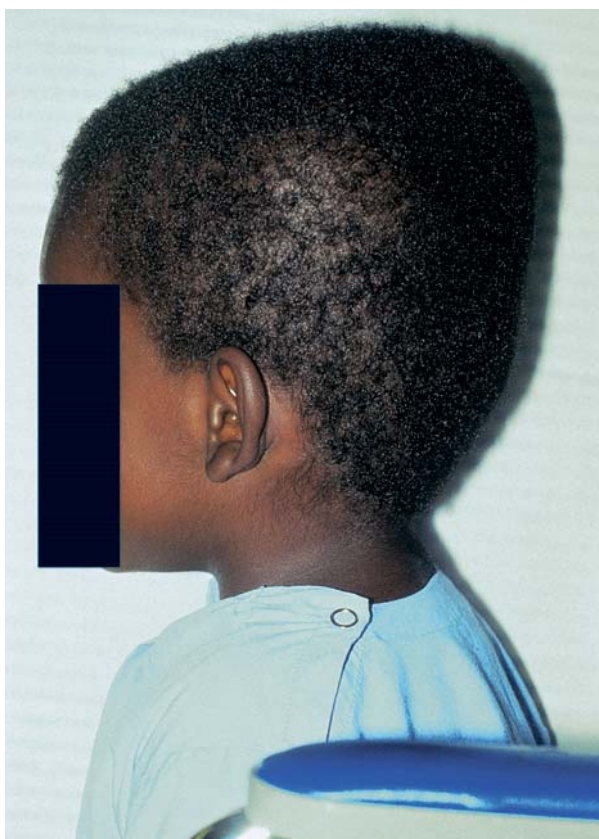


Fig. 1.56 Turricephaly from craniosynostosis.



Fig. 1.58 Radiograph of sagittal craniosynostosis showing absent suture lines with sclerosis and abnormal head shape.

Look at the mouth and palate. Submucous cleft palate may be revealed only by palpation. Any abnormalities of the midline are especially significant as they may indicate an associated abnormality of the pituitary gland (**Fig. 1.65**). Holoprosencephaly with microcephaly, hypotelorism and palatonasal abnormalities is due to a mutation of a midline patterning gene and there will be failure of fusion of the midline cerebral structures, often with associated hypopituitarism



Fig. 1.59 Severe hypotelorism.

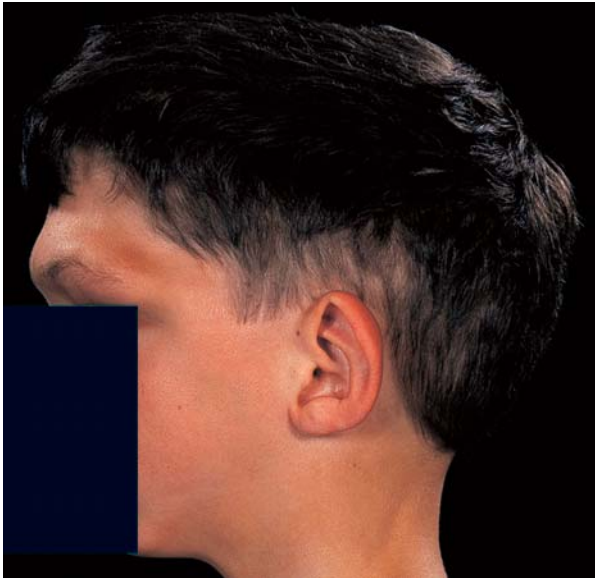
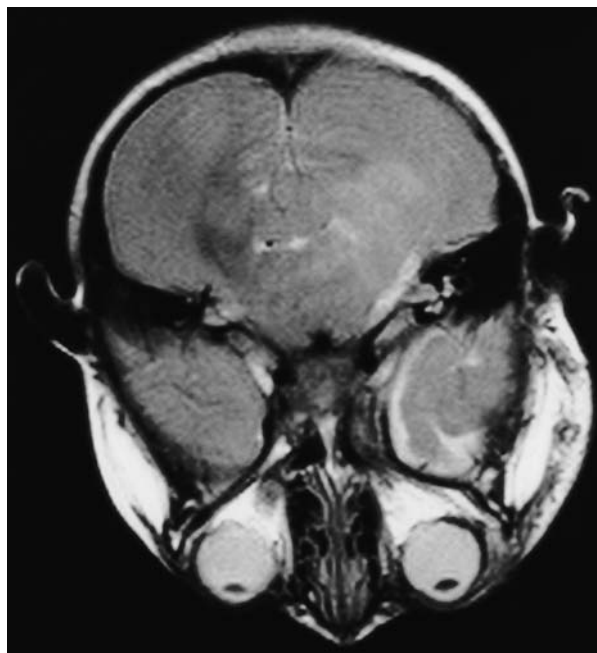


Fig. 1.60 Heavy supraorbital ridges in frontometaphyseal dysplasia.



Fig. 1.61 Ptosis, seen in 25% of girls with Ullrich–Turner, the majority of children with Noonan syndrome, and more than 50 other dysmorphic syndromes.



Figs 1.63, 1.64 Exophthalmos in neurofibromatosis (left) secondary to prolapsing temporal horn into orbit (right).

Fig. 1.62 Exophthalmos in thyrotoxicosis.



(Figs 1.66 & 1.67). A less severe but related abnormality produces the single central incisor and growth hormone deficiency syndrome (Fig 1.68).

Cleft palate is part of the Smith–Lemli–Opitz syndrome, in which there may be associated genital ambiguity (Fig. 1.69). A high arched palate may be seen

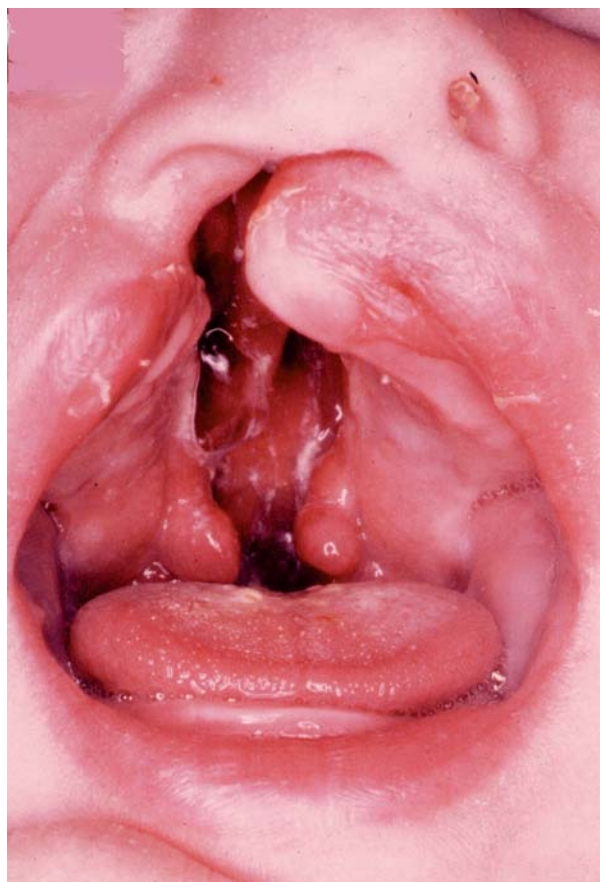


Fig. 1.65 Cleft lip and palate, in this case associated with panhypopituitarism.

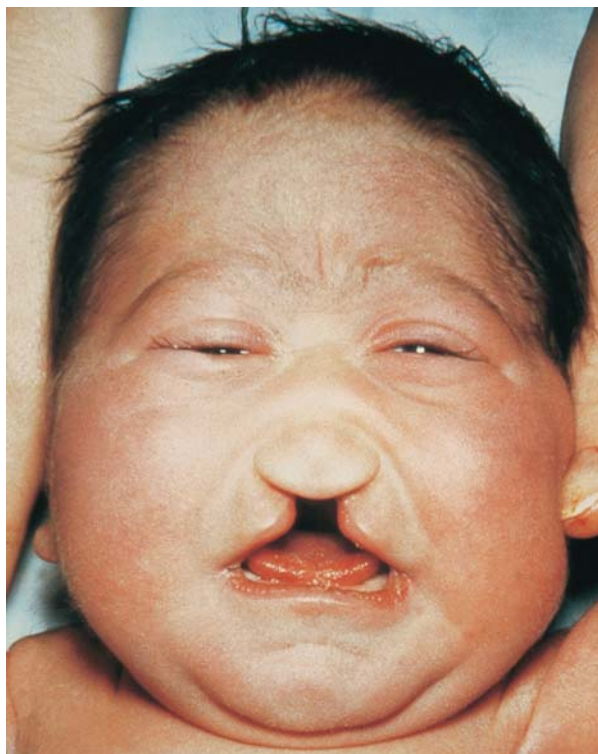


Fig. 1.66 Midline cleft and abnormal nose in holoprosencephaly. There may be associated panhypopituitarism.

in the Marfan, the Ullrich–Turner and some other dysmorphic syndromes (**Fig. 1.70**).

The tongue is smooth (**Fig. 1.71**) in iron deficiency of any cause and, in older age groups, in pernicious anemia, where it may be associated with other autoimmune disease. Both the tongue and lips may show neuromata in neurofibromatosis and in the multiple endocrine neoplasia (MEN) type IIb syndrome (**Fig. 1.72**). The lips may be swollen and ‘fish-like’ in Crohn’s disease (**Fig. 1.73**) and MEN-IIb. Oral candidiasis outside the neonatal period (**Fig. 1.74**) may signal type I diabetes mellitus, immunodeficiency associated with hypoparathyroidism in DiGeorge syndrome and the autoimmune polyglandular type I or ‘HAM’ syndrome of hypoparathyroidism, adrenal failure and moniliasis.

The teeth may be unusually soft and carious in disorders affecting collagen, fibrin and calcium metabolism, and peg-like in ectodermal dysplasia (**Fig. 1.75**). They are an abnormal shape in the Rubinstein–Taybi syndrome (**Fig. 1.76**). They may be stained or rotted

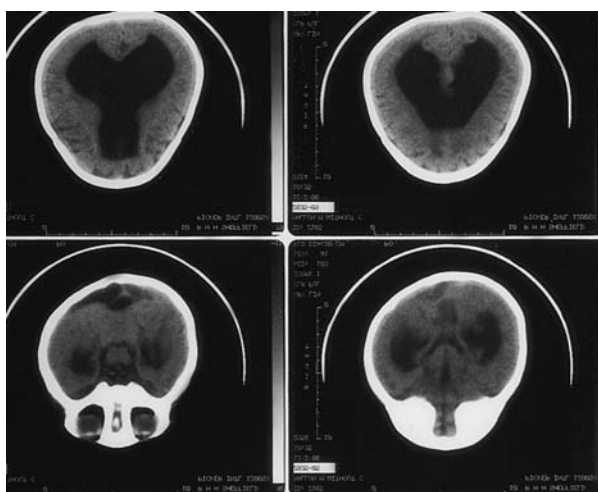


Fig. 1.67 Computed tomogram of the patient in Fig. 1.66, demonstrating abnormal midline structures and cloverleaf ventricles.

by drugs and bilirubin (**Fig. 1.77**). After chemotherapy for malignancy there may be enamel hypoplasia (**Fig. 1.78**). An assessment of the presence and number of the primary dentition and appearance of

Fig. 1.68 Single central incisor, associated with congenital growth hormone deficiency.



Fig. 1.70 High arched palate seen in 75% of girls with Ullrich–Turner syndrome and in most patients with Marfan syndrome.



Fig. 1.71 Smooth tongue in severe iron deficiency.



Fig. 1.69 Isolated cleft palate in Smith–Lemli–Opitz syndrome.



Fig. 1.72 Labial and glossal neuromas in MEN type IIb.

Fig. 1.73 'Fish lips' in oral Crohn's disease; similar swelling can be seen in MEN-IIb without the buccal ulceration.



the secondary teeth may give clues to skeletal age and physiological maturity (see below). Delayed eruption of the teeth is seen in any disorder that delays physical maturation (especially chronic disease, hypothyroidism and hypopituitarism), in cleidocranial dysostosis



Fig. 1.74 Oral candidiasis. If seen outside infancy, diabetes mellitus, immunodeficiency and autoimmune disease need to be excluded.



Fig. 1.77 Bilirubin staining after severe jaundice in an ex-premature neonate with sustained growth failure.



Fig. 1.75 Peg-like teeth in ectodermal dysplasia.



Fig. 1.76 Abnormal shaped teeth in Rubinstein-Taybi syndrome.



Fig. 1.78 Enamel hypoplasia secondary to chemotherapy.

(**Fig. 1.79**) and in some other dysmorphic syndromes associated with short stature. Early loss of teeth is seen in Down and Ehlers-Danlos syndromes.

The ears are low set with or without rotation (**Fig. 1.80**), or folded in an abnormal manner (**Fig. 1.81**) in a host of dysmorphic syndromes associated with short stature.

Head hair may be abnormally sparse or curled in several syndromic and metabolic disorders, and in progeria (**Fig. 1.82**). It may show abnormal patterns of whorl formation with underlying CNS malformation. Alopecia may indicate autoimmune disease (**Fig. 1.83**) and temporal hair loss is a feature of hypothyroidism (**Fig. 1.84**).

Palpation of the neck, from behind the patient, will allow assessment of the size and shape of the thyroid gland, which should also be measured at its widest point across the isthmus and from top to base on both sides of the midline. Most goiters in childhood (see Ch. 9) are smooth, although nodular enlargement



Fig. 1.79 Extreme delay of dental eruption is seen in cleidocranial dysostosis (severe hypothyroidism may produce similar delay).



Fig. 1.80 Low-set, backward, rotated ears – a non-specific finding in many dysmorphic syndromes.

may rarely occur. They move upwards on swallowing and it is useful to have a glass of water in the examination room for this purpose. Aberrant lingual thyroid tissue may be visible in the mouth at the root of the tongue on swallowing (**Fig. 1.85**). Retrosternal thyroid tissue can be identified by ultrasonography or lateral radiography of the thoracic inlet. Thyroglossal cysts are usually near the midline, solitary and transilluminate (**Fig. 1.86**).



Fig. 1.81 Abnormal helical pattern of ear in pseudohypoparathyroidism.



Fig. 1.82 Sparse head hair in the Russell-Silver syndrome



Fig. 1.83 Alopecia areata in autoimmune disease.

THE CHEST, ABDOMEN AND CARDIOVASCULAR SYSTEM

These systems should be examined to exclude any organic disorders that could produce poor growth or mimic an endocrinopathy. It is especially important to measure the blood pressure, as hypertension may be a feature of pheochromocytoma, CNS tumors, neuro-



Fig. 1.84 Temporal thinning of the hair in severe hypothyroidism.



Fig. 1.85 Goitrous lingual thyroid.

fibromatosis, the Cushing and Conn syndromes, ovarian tumors and some disorders of adrenal steroid biosynthesis. Hypertension in the right arm is also a feature of coarctation of the aorta, which may be present in 40% of girls with Ullrich–Turner syndrome, and so the femoral pulses must also be assessed. A wide pulse pressure (with tachycardia) is a feature of thyrotoxicosis. Low blood pressure with postural hypotension can be seen in adrenal insufficiency.

Major heart malformations and abnormal chest shape, such as pectus excavatum or pectus carinatum (Figs 1.87 & 1.88), may be seen in many syndromes associated with both short and tall stature. A rachitic rosary may be seen in vitamin D deficiency (see Fig. 11.24). Many of the storage disorders, syndromic malformations, and disorders of bone and collagen metabolism may show a scoliosis or kyphoscoliosis (Fig. 1.89). There is an accentuated lumbar lordosis or gibbus in achondroplasia (Fig.



Fig. 1.86 Thyroglossal cyst.



Fig. 1.87 Pectus excavatum in the Marfan syndrome.

1.90). The degree of angulation of the spine can be assessed radiographically (Fig. 1.91) or by surface mapping techniques (Fig. 1.92), and the loss of height quantified by measurement of sitting height.

There may be abdominal organomegaly in some of the storage disorders, thalassemia and Beckwith–Wiedemann syndrome, where an umbilical hernia or

Fig. 1.88 Pectus carinatum in the Noonan syndrome.



Fig. 1.90 Lumbar gibbus in achondroplasia.



Fig. 1.89 Scoliosis with plexiform neuroma in neurofibromatosis.



omphalocele can also be seen (**Fig. 1.93**) (see Ch. 3). Adrenal carcinomas producing virilization are often large and palpable (**Fig. 1.94**). Inspection of the anal margin may reveal signs of sexual abuse or chronic inflammatory bowel disease (**Fig. 1.95**).

THE BREASTS

Breast tissue and the pectoralis major muscle may be absent congenitally in the Poland sequence (**Fig. 1.96**) (there may also be associated heart, renal and vertebral defects). It may be damaged or destroyed after bilateral neonatal breast abscess (**Fig. 1.97**), or after surgery for abscess or physiologic neonatal gynecomastia (**Fig. 1.98**). Physiologic gynecomastia in the adolescent male is common and may be seen especially in the obese individual (**Fig. 1.99**). It is also



Fig. 1.91 Radiograph of scoliosis in camptodactyly syndrome of the Tel-Hashomer variety.

often unilateral (**Fig. 1.100**) and in any case may possibly require surgical resection and/or liposuction. Pathologic causes of early breast development are discussed in Chapter 6. Virginal breast hypertrophy (juvenile fibroadenoma) is uncommon but dramatic (**Fig. 1.101**). Accessory nipples are common (**Fig.**

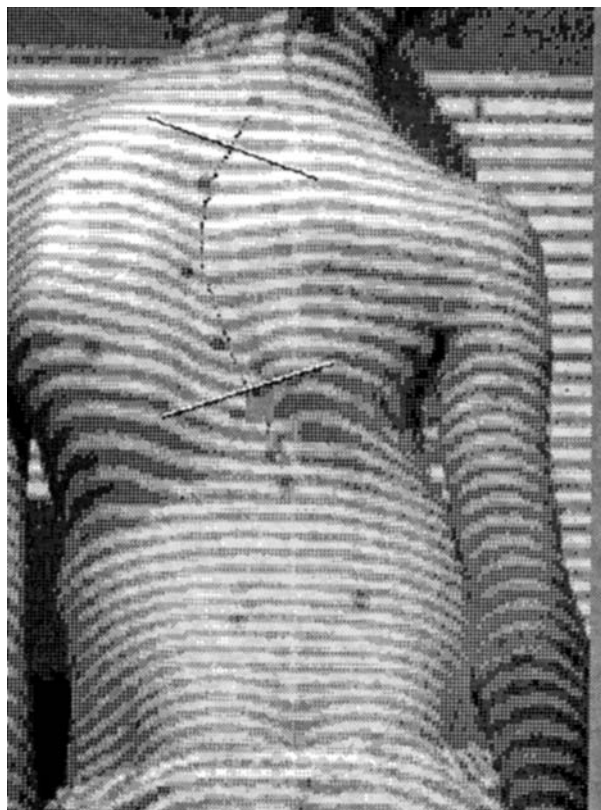


Fig. 1.92 Assessing scoliosis using optical surface mapping.



Fig. 1.94 Massive adrenal carcinoma presenting as abdominal mass with virilization.



Fig. 1.93 Umbilical hernia and visible organomegaly in Beckwith–Wiedemann syndrome.

1.102); it is rare, but possible, for them to overlie significant breast tissue.

THE GENITALIA

Many endocrine disorders have associated abnormalities of the genitalia; these are dealt with in detail in Chapters 6, 7 & 8.

In both sexes look especially for signs of hernia (or the scars of their repair early in life). In all patients



Fig. 1.95 (Left) Anal signs of Crohn's disease.

Fig. 1.96 (Bottom) Poland sequence. There is absence of the left pectoralis major and breast tissue. This child was referred with unilateral breast enlargement – a good example of normal stage 4 breast development.





Fig. 1.97 Neonatal breast abscess. Delayed antibiotic therapy or mistaken surgical intervention can lead to later amastia.



Fig. 1.100 Unilateral male gynecomastia, not uncommon but difficult to explain in the absence of a history of trauma.



Fig. 1.98 Physiologic neonatal gynecomastia.



Fig. 1.101 Virginal breast hypertrophy (juvenile fibroadenoma).



Fig. 1.99 Male gynecomastia with moderate obesity.



Fig. 1.102 Accessory nipple.

	Male	Female
Pubic hair		
1	None	None
2	Barely visible at base of penis or on scrotum	Barely visible on mons or labia
3	More visible, darker, same sites as (2)	More visible, darker, same sites as (2)
4	More extensive and dark, extending to suprapubic region	More extensive and dark, extending to suprapubic region
5	Adult triangle with extension on to medial aspect of thighs	Adult triangle
5+	Extension upwards in midline	Extension upwards in midline and on to medial aspect of thighs
Male genital stages		
1	Prepubertal penis	
2	Beginning of enlargement, more in length than breadth. Scrotal skin thickens	
3	Further enlargement and early separation of contour of glans from shaft	
4	Near adult shape, not fully grown. Scrotal skin dark and thick	
5	Adult penis	
Testicular volume	Recorded directly by comparison to an orchidometer (Fig. 1.105). Onset of puberty (≥ 3.5 mL testis) is followed by the onset of the pubertal growth spurt after approx. 6 months. Peak height velocity is attained with 12–14 mL testicular volume	
Female breast stages		
1		Prepubertal
2		Breast bud palpable
3		Obvious elevation of breast tissue
4 ^a		Areola and nipple separate on enlarging breast
5		Adult size and shape; areola and nipple merge
Menarche		Recorded as an all-or-nothing event (although regular periods may take time to establish)
Growth potential (cm)		
Stage 2 – PHV	12.5 (2.9–28.7)	6.8 (0.0–16.3)
Stage 2 – final	27.9 (17.9–41.2)	21.0 (11.6–29.4)
Stage 3 – final	20.3 (3.9–30.1)	13.7 (6.1–21.6)
PHV – final	15.7 (9.6–22.6)	14.4 (8.6–23.0)
Stage 4 – final	14.6 (1.1–25.2)	7.5 (2.7–13.7)
Stage 5 – final	8.4 (0.0–20.5)	3.8 (0.0–10.0)
Menarche – final	–	5.8 (1.0–12.7)
^a Some normal girls will not pass this stage of development. The onset of the pubertal height spurt is concurrent with the appearance of stage 2 breast development, and peak height velocity (PHV) is usually associated with stage 3 breast development.		
^b Values are mean (range) for stage of puberty. To convert centimeters to inches, multiply by 0.394. Data from J.M.H. Buckler, with permission.		

Table 1.2 Stages of sexual maturation

presenting with a possible endocrine disorder, a full assessment of physical maturity is mandatory. It is usual to stage the appearance of the pubic hair, penis and testicular volume in the male, and the appearance of the breast, pubic hair and the onset of menstruation in a girl. Details of this staging are given in **Table 1.2** and **Figs 1.103–106**.

Other secondary sexual characteristics should be noted, such as acne (**Fig. 1.107**), axillary hair, vaginal discharge and an adult body odor. Any discrepancy between the stages of sexual development in an individual is of particular importance (**Figs 1.108 & 1.109**) (see Ch. 6).

Shawl scrotum, where the root of the penis lies within the upper scrotum, which is often bifid (see Ch. 8), is seen in several dysmorphic syndromes, including the Aarskog syndrome. Other apparently minor abnormalities of genital architecture may have significance in the context of other physical findings.

CENTRAL NERVOUS SYSTEM AND EYES

Examination here should concentrate on an assessment of developmental or educational level and an exclusion of major neurologic abnormality. It is particularly important to examine the optic discs, which might demonstrate

Fig. 1.103 Female pubic hair, stages 1–5+.

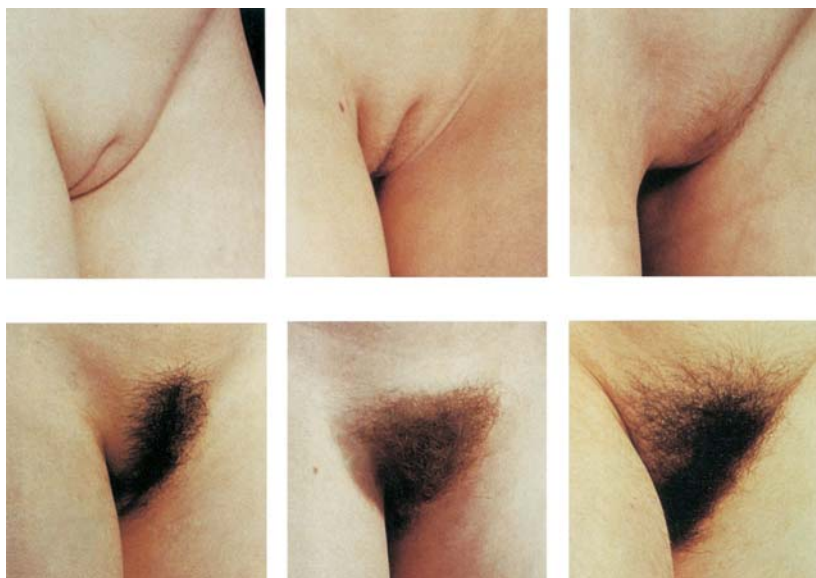
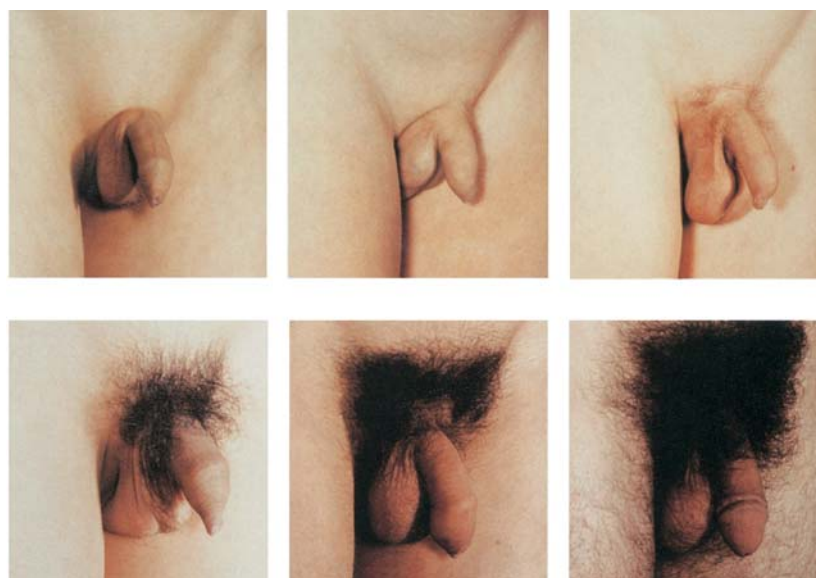


Fig. 1.104 Male penis and pubic hair development, stages 1–6.



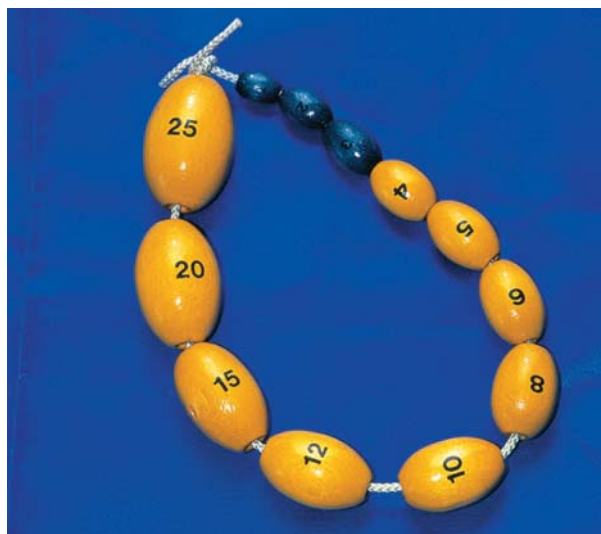


Fig. 1.105 Prader orchidometer graded from 1 to 25 mL. The achievement of pubertal 4-mL testes is shown by a change from blue to yellow beads.



Fig. 1.107 Early acne in a 2-year-old child with precocious puberty.

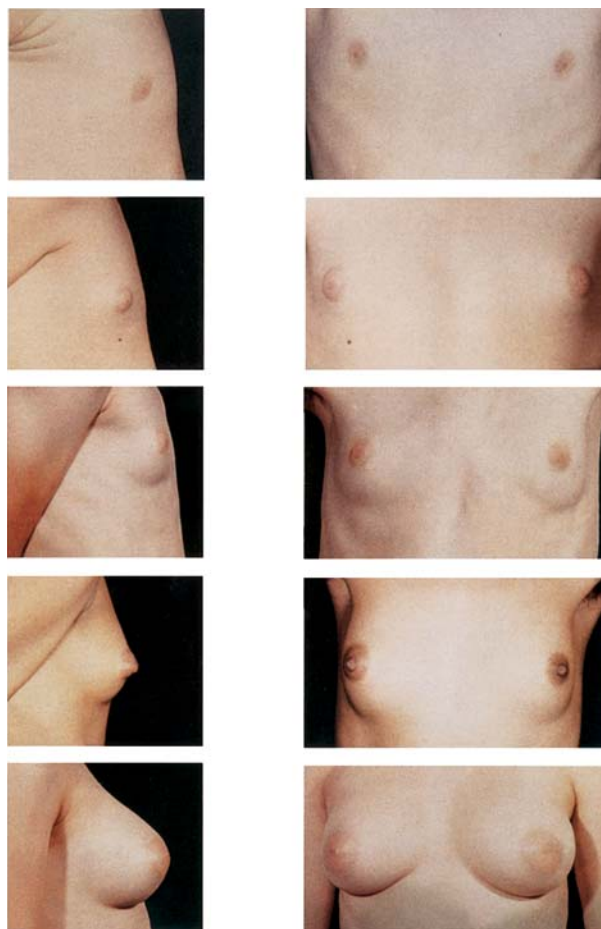


Fig. 1.106 Female breast development, stages I–5.



Fig. 1.108 Excess adrenal steroids – acne and axillary hair are excessive for the stage of breast development.



Fig. 1.109 Ovarian tumor with breast development in the absence of any pubic hair.

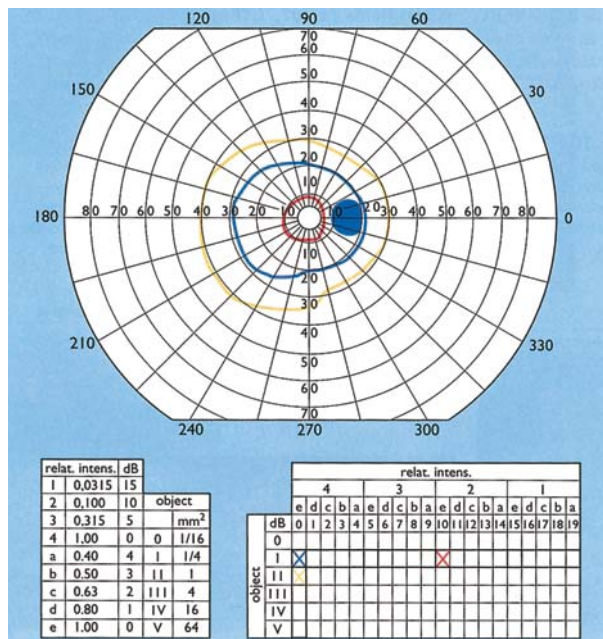
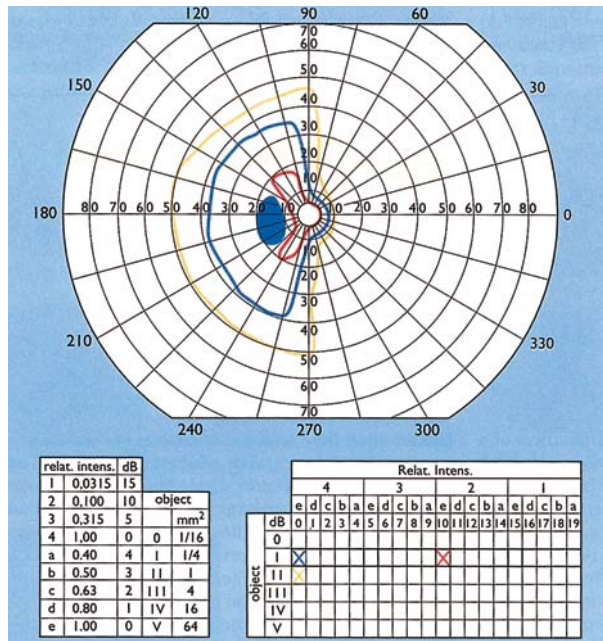
papilledema (**Fig. 1.110**) secondary to raised intracranial pressure. Growth hormone therapy may occasionally result in benign raised intracranial hypertension that results in dramatic papilledema. The pallor of optic atrophy (**Fig. 1.111**) may be secondary to compression by a local tumor or raised intracranial pressure, or found in the DIDMOAD syndrome of Diabetes Insipidus, Diabetes Mellitus, Optic Atrophy and Deafness (see Ch. 10). The visual fields (**Figs 1.112 & 1.113**) may show bitemporal restriction in the presence of compression of the optic chiasm by a craniopharyngioma. The retina may be dysplastic with small optic nerve heads in septo-optic dysplasia (**Figs 1.114–1.116**) associated with panhypopituitarism or isolated pituitary hormone deficiencies and/or midline brain abnormalities.



Fig. 1.110 Papilledema in craniopharyngioma.



Fig. 1.111 Optic atrophy, as seen in optic nerve compression or DIDMOAD syndrome.



Figs 1.112, 1.113 Visual fields in a child with craniopharyngioma – temporal hemianopia in the left eye (top) and generalized restriction of vision in the right eye (bottom) secondary to compression of the optic chiasm. This formal plotting is possible in older, cooperative children. In the young child the presence of temporal field loss can be demonstrated by confrontation or by bringing a small, interesting, object inwards from the periphery, close to the child's face and noting when there is a reaction.

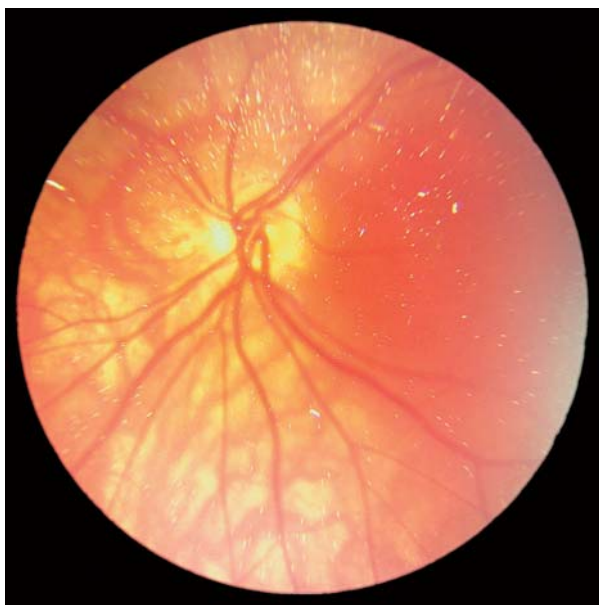


Fig. 1.114 Retinal dysplasia in septo-optic dysplasia (de Morsier syndrome).

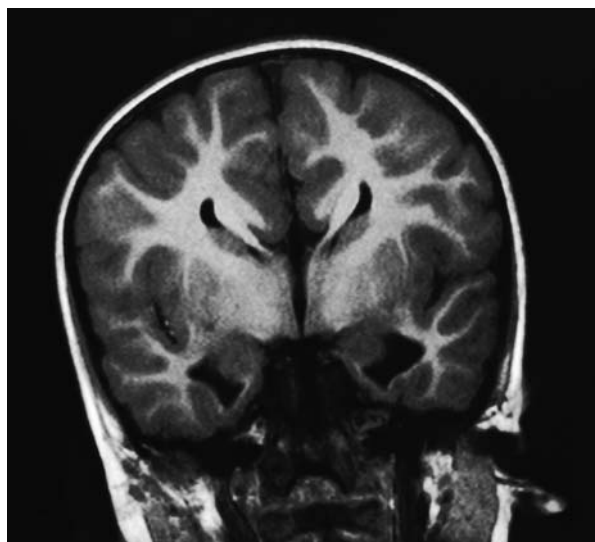


Fig. 1.116 Absent corpus callosum in septo-optic dysplasia – MRI view.

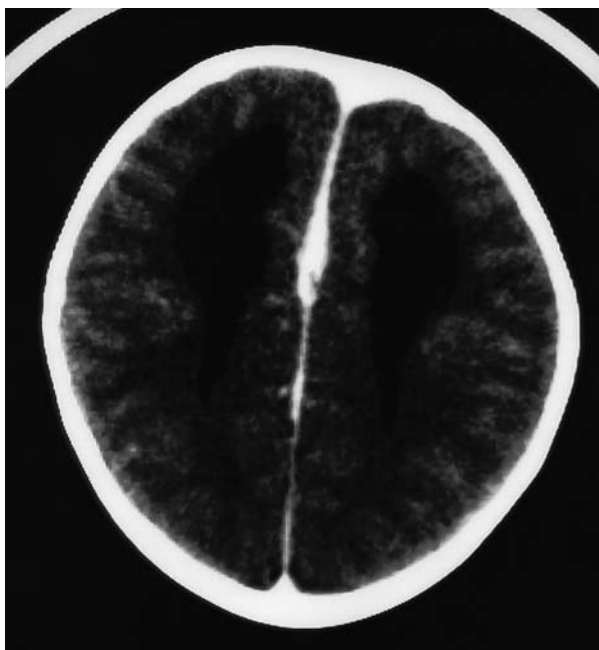


Fig. 1.115 Absent midline structures in the patient in Fig. 1.114; CT scan showing parallel ventricles.

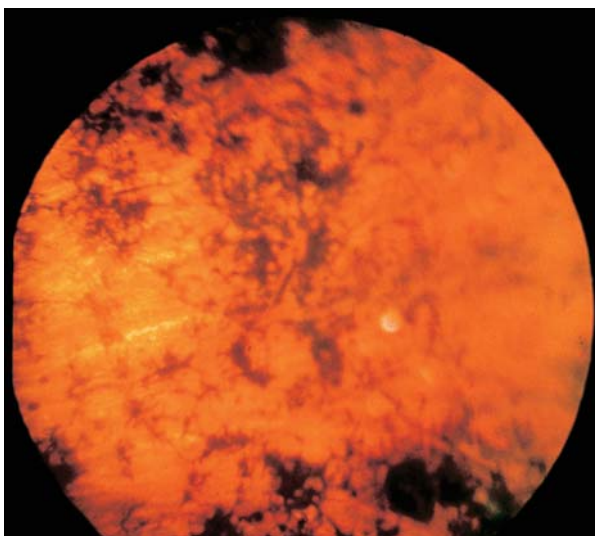


Fig. 1.117 Retinitis pigmentosa, in the Laurence–Moon syndrome.

Retinitis pigmentosa (**Fig. 1.117**) is seen in several syndromes associated with short stature, for instance the Laurence–Moon (with obesity, spasticity, learning difficulties and hypogonadism) or similar Bardet–Biedl (with obesity, polydactyly, learning difficulties and

hypogonadism) syndromes. Storage deposits may be visible in either the retina (**Fig. 1.118**) or lens. The lens shows dislocation or loose fixation in the Marfan syndrome (said to be more commonly upwards) and in homocystinuria (said to be more commonly downwards) (**Fig. 1.119**).

The eyes might show abnormal blue coloration of the cornea in disorders of collagen formation, such as osteogenesis imperfecta (**Fig. 1.120**). A nevus of Ota can be associated with intracranial hamartomas and



Fig. 1.118 Pseudopapilledema caused by abnormal storage deposits in geleophysic dwarfism.

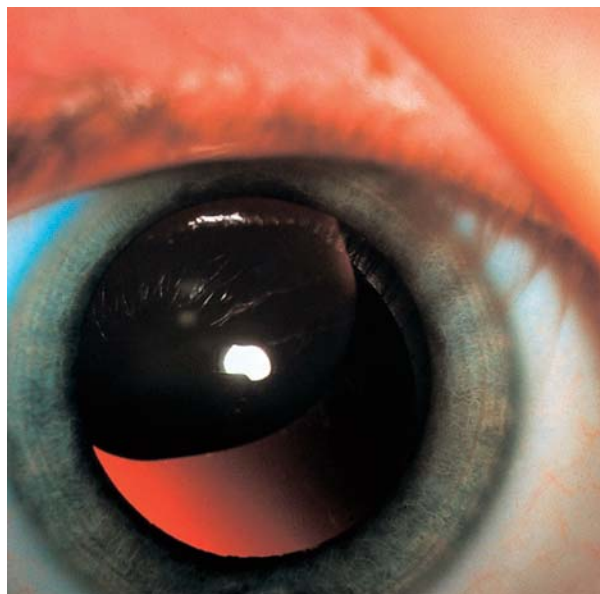


Fig. 1.119 Upward lens dislocation in the Marfan syndrome.

sexual precocity (**Fig. 1.121**). Heterochromia is seen in several syndromes associated with short stature and hypogonadism (**Fig. 1.122**). There may be abnormal sparsity, duplication or luxuriance of the eyelashes in several short stature syndromes and in severe chronic ill health (**Fig. 1.123**).



Fig. 1.120 Blue sclerae in the commonest (type I) osteogenesis imperfecta.



Fig. 1.121 Nevus of Ota, in this case associated with gigantism and sexual precocity due to hypothalamic dysfunction.



Fig. 1.122 Heterochromia.



Fig. 1.123 Long eye lashes in De Lange syndrome.



Fig. 1.124
Abnormal dimpled abdominal fat in hypopituitarism.



Fig. 1.125
Generalized left-sided hemihypertrophy.



Fig. 1.126
Isolated hemihypertrophy of right leg.

BODY SHAPE AND THE SKIN

Look at the general shape of the body and at the distribution of muscle and fat. Abnormal muscularity may be seen in non-salt-losing males with the adrenogenital syndrome and in anabolic steroid abuse in young adolescents. Generalized lipodystrophy is seen in progeria and in the 'leprechaun' and related syndromes, where there may be associated insulin resistance (see Ch. 4); there are also some localized lipotrophy syndromes, which can be both congenital and acquired (and may be related in the latter case to glomerulonephritis and protease inhibitors for treating human immunodeficiency virus).

Localized lipotrophy is seen in relation to injection sites of (usually) animal insulin and lipohypertrophy in relation to human insulin and growth hormone (see Ch. 10). Excess adiposity is a feature of many endocrine

disorders and may show a peculiar dimpled appearance in hypopituitarism (Fig. 1.124).

Hemihypertrophy may affect the whole body (Figs 1.125 & 1.127) or isolated areas such as one side of the face or one limb (Fig. 1.126). Asymmetry is associated with Russell–Silver syndrome and Beckwith–Wiedemann syndrome, and in the isolated form may also increase the risk of Wilms tumor. Hemiatrophy may be seen in VATER syndrome (Fig. 1.127). Local hypertrophy of a limb in association with hemangiomas

Fig. 1.127

Hemiatrophy in
Vertebral Anal
Tracheoesophageal
fistula Renal
abnormalities
(VATER) syndrome.

**Fig. 1.128** Limb overgrowth in Klippel–Trenaunay–Weber syndrome.

(Klippel–Trenaunay–Weber syndrome) may also occur (Fig. 1.128), as well as in association with Proteus syndrome and its related conditions (Fig. 1.129) (see also Ch. 3).

Neurofibromatosis (see Chs 2 & 6) is signaled by a large number of café-au-lait spots, axillary freckling (Fig. 1.130) and neuromas (Fig. 1.131) – usually

**Fig. 1.129** Linear pigmentation in the Proteus syndrome, overgrowth of left foot.**Fig. 1.130** Café-au-lait spots in neurofibromatosis. Note the relatively smooth outline.



Fig. 1.131 Multiple neuromas in neurofibromatosis.

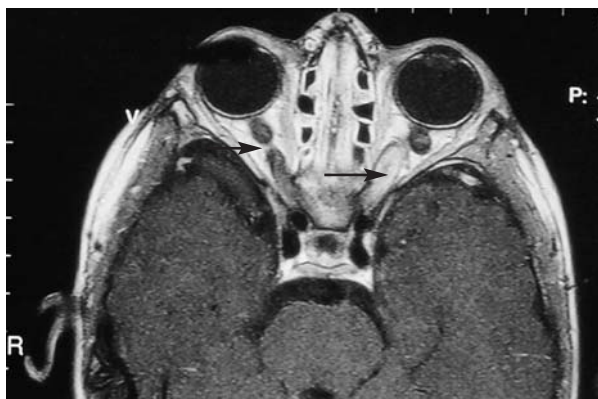


Fig. 1.134 Optic gliomas in neurofibromatosis involving both optic nerves.



Fig. 1.132 Plexiform neuroma in neurofibromatosis.



Fig. 1.135 Café-au-lait spot in McCune–Albright syndrome. Note irregular border.

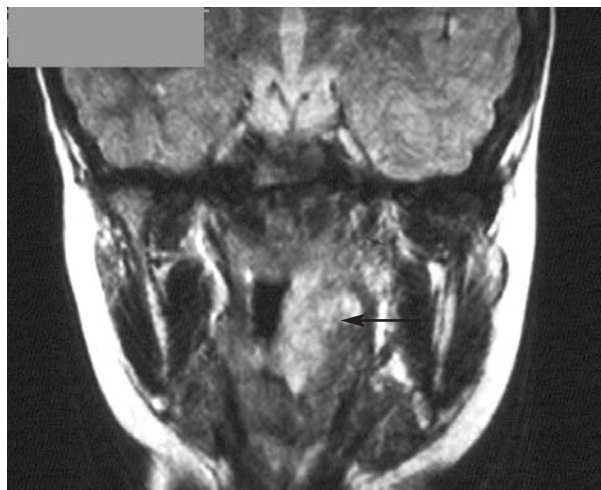


Fig. 1.133 Internal plexiform neuroma invading thoracic inlet.

more often in young adult life, although small or solitary neuromas may be palpated in young children. The café-au-lait patches may be discrete or large and plexiform (**Fig. 1.132**), and may then be external or involve deeper structures (**Figs 1.63, 1.64, 1.89 & 1.133**). There may be unilateral or bilateral optic gliomas (**Fig. 1.134**) with reduced visual fields, disk pallor or sexual precocity (see Ch. 6). The edge of these spots is said to be relatively smooth, like the coastline of California. The café-au-lait spot in McCune–Albright syndrome (**Fig. 1.135**) associated with sexual precocity (see Ch. 6) has a rough outline like the coast of Maine. Multiple pigmented nevi (**Fig. 1.136**) are associated



Fig. 1.136 Multiple pigmented nevi, here associated with Ullrich–Turner syndrome.

Fig. 1.137

Segmental nevi in Turner syndrome indicating tissue mosaicism. A similar appearance with café-au-lait spots can be seen in segmental neurofibromatosis.



Fig. 1.138

Generalized hyperpigmentation in Nelson syndrome.



with the Ullrich–Turner syndrome and a number of syndromic malformations and neuroectodermal tumors. Nevi and café-au-lait spots may show a segmental distribution, indicating tissue mosaicism (**Fig. 1.137**).

Skin pigmentation may be abnormally increased with oversecretion of adrenocorticotrophic hormone (ACTH) as in Addisonism and Nelson syndrome (see Chs 2 & 11), and this may be generalized (**Fig. 1.138**) or localized to scar tissue (**Fig. 1.139**). Coal-black discoloration of the axillae or neck (**Fig. 1.140**) (acanthosis nigricans) is associated with insulin resistance and obesity (see Chs 5 & 10). Vitiligo (**Fig. 1.141**) is commonly an isolated disorder but may be associated with several of the polyglandular syndromes (see Ch. 11).



Fig. 1.139 Scar pigmentation in Addison's disease.



Fig. 1.140
Axillary acanthosis nigricans associated with insulin resistance.



Fig. 1.142
Tissue paper scars from excess skin fragility in Ehlers–Danlos syndrome.

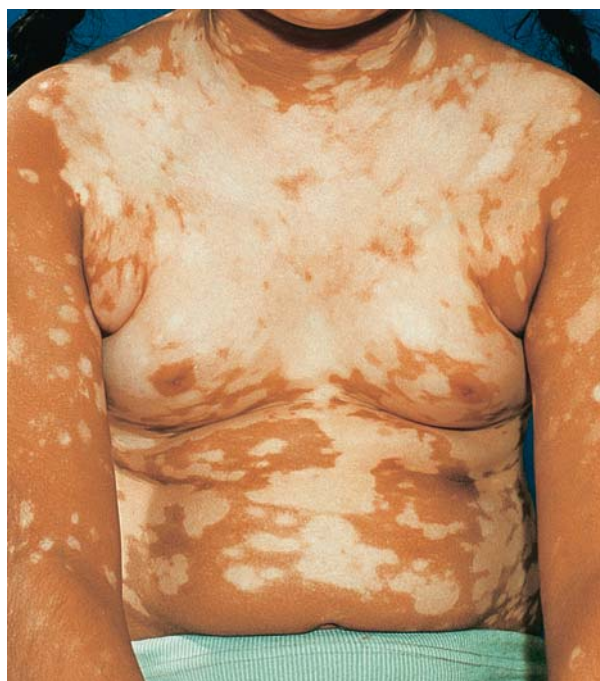


Fig. 1.141 Severe vitiligo in polyglandular syndrome type I.



Fig. 1.143
Extensible skin in Ehlers–Danlos syndrome.

Easy bruising and skin fragility are seen in the tissue paper scarring of Ehlers–Danlos syndrome (**Fig. 1.142**), where there is also increased skin and joint laxity (**Figs 1.143 & 1.144**). Non-accidental bruising and burns indicate physical abuse (**Fig. 1.145**).

The Cushing syndrome in childhood is often associated with easy bruising. A particular feature of childhood-onset Cushing syndrome is marked hirsutism

(which is also a feature of other disorders of the adrenal gland and ovary characterized by overproduction of testosterone; see Chs 3, 6, 8 & 11). Hirsutism is also seen as part of the fetal alcohol syndrome (see below). Treatment with some drugs, such as metyrapone, can also cause hirsutism. The use of diazoxide in hyperinsulinism (**Fig. 1.146**) (see Ch. 11) causes hypertrichosis (generalized and non-pigmented). Retention of excess lanugo hair may be seen in Aarskog syndrome (**Fig. 1.147**) and in anorexia nervosa. Striae are a feature of especially iatrogenic Cushing syndrome

Fig. 1.144
Hypermobile
joints in
Ehlers–Danlos
syndrome.



Fig. 1.146 Hypertrichosis secondary to diazoxide treatment. Also seen with ciclosporin.

Fig. 1.145 Child abuse. Multiple bruises. (Note characteristic shortened lower body segment which may mimic hypochondroplasia.)



Fig. 1.147
Downy body hair
in the X-linked
recessive Aarskog
syndrome
associated with
short stature.



(**Fig. 1.148**) and may be also seen in nutritional obesity and in tall stature (see Chs 3 & 5).

Dry skin is seen in atopic disorders, ectodermal dysplasia and some other dysmorphic syndromes. Excessive lichenification is seen in the X-linked metabolic disorder placental sulfatase deficiency (**Fig. 1.149**) when the affected fetus will be post-mature and maternal

estriol levels will have been undetectable during pregnancy. Dry fissured reddening of the palms and soles is seen in the 3A syndrome of **adrenal** failure, **alacrima** and **achalasia**, where there may also be



Fig. 1.148 Striae in iatrogenic Cushing syndrome.



Fig. 1.149 Ichthyotic skin in placental sulfatase deficiency.



Fig. 1.150 Red fissured feet in the 3A syndrome.

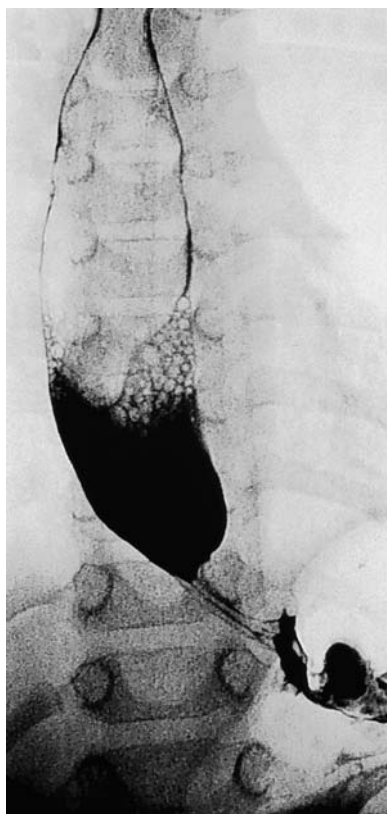


Fig. 1.151
Achalasia in the
3A syndrome.



Fig. 1.152 Dimpling over tibia in hypophosphatasia.

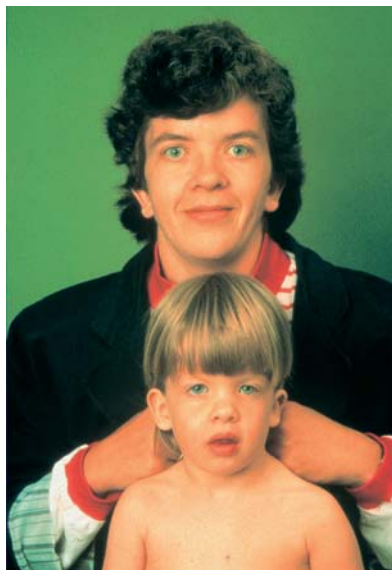
progressive nerve degeneration (**Figs 1.150 & 1.151**). Necrobiosis lipoidica and granuloma annulare have associations with insulin-dependent diabetes mellitus (see Ch. 10). Dimpling of the skin is seen in hypophosphatasia, where there is undermineralization of the skeleton and teeth and, in the childhood form, short stature (**Fig. 1.152**).

THE PARENTS

It is important to examine the parents briefly, if at all possible; they may provide valuable clues as to

Fig. 1.153

Familial Noonan syndrome in parent and child.



Auxology (including parents) and bone age
 Any abnormalities of the hands, feet, nails or arms
 Any abnormalities of the head and neck (with special reference to the midline, mouth, tongue and thyroid)
 Any chest wall (including breast) or spine abnormalities
 Any cardiovascular or respiratory abnormalities
 Any abdominal abnormalities? (must include external genital inspection)
 Stage of sexual maturation
 Any abnormal skin or fat signs
 Any abnormal body shape or asymmetry
 Any eye abnormalities including lens, visual field and retina
 Any abnormal appearance of either of the parents

Table 1.3 Summary of essential points on physical examination**Fig. 1.154** Fetal alcohol syndrome in later childhood showing typical appearance of lower face.

the diagnosis. Many skeletal dysplasias and some dysmorphic syndromes associated with both tall and short stature are dominantly inherited, and may be more obvious in later life (**Fig. 1.153**). A parent, more often the mother, may show signs of undiagnosed hypothyroidism or hyperthyroidism, and the mother may be mildly affected by a metabolic disorder, such as phenylketonuria or myotonic dystrophy, which has affected the infant severely. A wide philtrum and a thin upper lip may be seen in the offspring of heavy drinkers during pregnancy, along with short stature, learning difficulties, hirsutism and limb abnormalities (**Fig. 1.154**).

The cardinal features to include in the examination of a child with a possible growth or endocrine disorder are summarized in **Table 1.3**.

**Fig. 1.155** Left hand and wrist radiograph for bone age estimation.

SKELETAL MATURITY

Although not strictly part of the examination of a child, it is pertinent to discuss a complementary, radiographic, means of establishing physiologic maturity. The most commonly used methods involve assessing the number and degree of development of the bones of the left hand and wrist (**Fig. 1.155**) (although other growth

centers can be used, including the jaw and teeth). Several methods exist for scoring or ‘aging’ the individual ossification centers in comparison to a standard atlas or by means of a computer recognition system. It is then possible by using published equations incorporating current height, or in some cases height

and recent height velocity, to calculate a predicted adult height (with a range of error of ± 2 SD). In this book the Tanner–Whitehouse 2 (TW2) method has been used in the creation of the charts, although an updated version (TW3) has recently become available.